

The Astrophysical Journal Letter Revised: 2002 March 24

A NEW METHOD TO CONSTRAIN THE IRON ABUNDANCE FROM COOLING DELAYS IN CORONAL LOOPS

Markus J. Aschwanden¹, Carolus J. Schrijver¹, Amy R. Winebarger^{2,3}, and Harry P. Warren³

ABSTRACT

Recent observations with TRACE reveal that the time delay between the appearance of a cooling loop in different EUV temperature filters is proportional to the loop length, $\Delta t_{12} \propto L$. We model this cooling delay in terms of radiative loss and confirm this linear relationship theoretically. We derive an expression that can be used to constrain the coronal iron enhancement $\alpha_{Fe} = A_{Fe}^{cor}/A_{Fe}^{Ph}$ relative to the photospheric value as function of the cooling delay Δt_{12} , flux F_2 , loop width w , and filling factor $q_w \leq 1$. With this relation we find upper limits on the iron abundance enhancement of $\alpha_{Fe} \leq 4.8 \pm 1.7$ for 10 small-scale nanoflare loops, and $\alpha_{Fe} \leq 1.4 \pm 0.4$ for 5 large-scale loops, in the temperature range of $T \approx 1.0 - 1.4$ MK. This result supports the previous finding that low-FIP elements, including Fe, are enhanced in the corona. The same relation constitutes also a lower limit for the filling factor, which is $q_w \geq 0.2 \pm 0.1$ and $q_w \geq 0.8 \pm 0.2$ for the two groups of coronal loops.

Subject headings: Sun: Corona — Sun: UV radiation

1. Introduction

Coronal EUV emission is mainly produced by radiative decay of collisionally excited, highly-ionized iron ions, i.e. by Fe^{8+} and Fe^{9+} in the 171 Å TRACE passband ($T \approx 1.0$ MK) and by Fe^{11+} at 195 Å ($T \approx 1.5$ MK). Coronal loops undergo various phases of heating and cooling. When steady heating operates, the loops evolve into a steady-state, where heating input is balanced by thermal conduction losses to the chromosphere and radiative losses into space, as described by the energy equation derived by Rosner, Tucker, & Vaiana (1978), generalized for gravity and non-uniform heating by Serio et al. (1981). When heating stops, coronal loops cool

¹Lockheed Martin Advanced Technology Center, Solar & Astrophysics Laboratory, Dept. L9-41, Bldg.252, 3251 Hanover St., Palo Alto, CA 94304, USA; e-mail: aschwanden@lmsal.com

²Computational Physics, Inc., 8001 Braddock Road, Suite 210, Springfield, VA 22151

³Naval Research Laboratory Code 7673, Washington DC 20375, USA

off by thermal conduction and radiative losses. One consequence of this cooling process is that the EUV emission peaks first in a high-temperature filter 1, e.g. in TRACE 195 Å, and later in a lower-temperature filter 2, e.g. in TRACE 171 Å, with a time delay that we call *cooling delay* Δt_{12} . This cooling delay was found to scale proportionally to the loop length L in a recent study (Winebarger et al. 2003). Under the assumption that the cooling time is dominated by radiative cooling, we can relate this observable time delay to the radiative loss function $\Lambda(T)$, which allows us to constrain the absolute abundances of iron ions, which dominates the radiative loss function in this coronal temperature range of $T \approx 1 - 2$ MK. The new method of determining iron abundances provides an important diagnostic for coronal heating mechanisms that involve preferential ion heating. This study demonstrates also that much more physical information can be inferred from the temporal evolution of the EUV intensity than from the intensity measured in a single image.

2. Theoretical Model

Plasma cooling through a narrow temperature range can be approximated by an exponential function,

$$T_e(t) = T_1 \exp\left(-\frac{t}{\tau_{cool}}\right), \quad (1)$$

where T_1 is the initial temperature at time $t = 0$ and τ_{cool} is the cooling time. Cooling over large temperature ranges would require the full consideration of the hydrodynamic equations, but the exponential approximation is fully justified for the narrow temperature range of $T_e \approx 1.0 - 1.4$ MK we are considering here, during the cooling of coronal flare loops through the two TRACE 171 and 195 Å filters (see also measurements in Warren et al. 2003). So, when a cooling plasma reaches the temperature T_1 of the peak response of the hotter filter ($T_1 = 1.4$ MK for TRACE 195 Å), the time delay Δt_{12} to cool down to the cooler filter T_2 (e.g. $T_2 = 0.96$ MK for 171 TRACE Å), can be expressed with Eq.1 as

$$\Delta t_{12} = t_2 - t_1 = \tau_{cool} \ln\left(\frac{T_1}{T_2}\right). \quad (2)$$

The cooling time scale could be dominated by thermal conduction losses in the initial phase, but is always dominated by radiative losses in the later phase (e.g., Antiochos & Sturrock 1982). Here we make the a priori assumption that the cooling of EUV loops in the $T_e \approx 1$ MK temperature range is dominated by radiative losses. This working hypothesis is particularly justified near the almost isothermal loop tops and is also corroborated by the observational result found in Aschwanden et al. (2000), where a median value of $\tau_{cool}/\tau_{rad} = 1.02$ was obtained from the statistics of 12 nanoflare loops observed with TRACE 171 and 195 Å. Moreover we show later that the radiative cooling time is always significantly shorter than the conductive cooling time for the cases analyzed here. Thus we set the cooling time τ_{cool} equal to the radiative cooling time τ_{rad} ,

$$\tau_{cool} \approx \tau_{rad} = \frac{E_{th}}{dE_R/dt} = \frac{3n_e k_B T_e}{n_e n_H \alpha_{FIP} \Lambda(T_e)} \quad (3)$$

where n_e is the electron density, n_H the hydrogen density, T_e the electron temperature, $k_B = 1.38 \times 10^{-16}$ erg K $^{-1}$ the Boltzmann constant, α_{FIP} the abundance enhancement factor for low *first-ionization potential* elements (at < 10 keV), and $\Lambda(T_e)$ the radiative loss function, which can be approximated with a constant in the limited temperature range of $T_e \approx 0.5 - 2.0$ MK, according to the piece-wise powerlaw approximation of Rosner et al. (1978), $\Lambda(T) \approx \Lambda_0 = 10^{-21.94}$ erg s $^{-1}$ cm 3 , for T=0.5-2.0 MK. The computation of the radiative loss function at a given temperature depends on the elemental atomic abundances, and thus we define a reference value $\Lambda_{0,Ph}$ for photospheric abundances. Coronal abundances generally show a density enhancement for low first-ionization potential (FIP) elements, which we express with an enhancement factor α_{FIP} . Since iron (Fe) contribution strongly at these temperatures, the radiative loss function in the corona scales as $\Lambda_{0,cor} = \Lambda_{0,ph} \times \alpha_{Fe}$. The cooling delay Δt_{12} as function of the coronal iron abundance α_{Fe} is thus (with Eqs. 1-3), assuming full ionization in the corona ($n_H = n_e$),

$$\Delta t_{12} = \frac{3k_B T_e}{n_e \alpha_{Fe} \Lambda_{0,Ph}} \ln \left(\frac{T_1}{T_2} \right). \quad (4)$$

When a loop cools through a passband, the maximum of the flux $F(t)$ is detected at the time when the loop temperature matches the peak of the response function, so the peak flux F_2 of the light curve in the lower filter corresponds to the emission measure EM at the filter temperature T_2 ,

$$F_2 = EM \times R_2 = (n_e^2 w q_w) \times R_2 \quad (5)$$

with the flux F_2 in units of DN/(pixel s), w is the loop width or diameter, q_w is the linear filling factor in case of unresolved substructures, and R_2 is the response function, which is $R_2 = 0.37 \times 10^{-26}$ cm 5 DN/(pixel s) for 171 Å and photospheric abundances (see Appendix A in Aschwanden et al. 2000). The value R_2 of the response function refers to the time at the beginning of the mission, while the degradation decreased this value by a factor of 0.78 in August 1999, the latest date of analyzed observations used here. The corresponding correction by a factor of $\geq \sqrt{0.78} = 0.88$ is neglected in the numerical values given in Table 1. Inserting the density from Eq.(5) into Eq.(4) we find the following expression for the iron abundance α_{Fe} ,

$$\alpha_{Fe} = \frac{3k_B T_2}{\Lambda_{0,Ph} \Delta t_{12}} \sqrt{\frac{R_2 w q_w}{F_2}} \ln \left(\frac{T_1}{T_2} \right) = 4.17 \left(\frac{w q_w}{1 \text{ Mm}} \right)^{1/2} \left(\frac{F_2}{10 \text{ DN/s}} \right)^{-1/2} \left(\frac{\Delta t_{12}}{1 \text{ min}} \right)^{-1}. \quad (6)$$

For a filling factor of unity ($q_w = 1$), the iron enhancement factor can be determined with an accuracy of about $\lesssim 20\%$, because the observables w , F_2 , and Δt_{12} can each be measured better than $\lesssim 10\%$. In case of unresolved fine structure, i.e. filling factors of $q_w < 1$, we obtain with Eq.(6) an upper limit for the iron enhancement.

Recent EUV observations with TRACE have shown that the cooling delay Δt_{12} is roughly proportional to the loop length L . In order to understand such a correlation we use the energy balance equation, which is valid in a steady-state, e.g., before the cooling process, at the turning point from dominant heating to dominant cooling, or at the turning point from dominant

conductive cooling to radiative cooling. The resulting scaling law is according to Rosner et al. (1978),

$$T_{max} \approx 1400(p_0 L)^{1/3} \times q_{Serio} \quad (7)$$

with p_0 the pressure and L the loop half length. This scaling law has been generalized for gravity and non-uniform heating by Serio et al. (1981), modified by the correction factor

$$q_{Serio} = \exp \left(-0.08 \frac{L}{s_H} - 0.04 \frac{L}{s_p} \right), \quad (8)$$

where s_H is the heating scale length and $s_p = 47,000 \times T_{MK}$ km the pressure scale height.

With the ideal gas law ($p = 2n_e k_B T_{max} = p_0 q_p$), corrected for the pressure at the loop top [$q_p = \exp(-h/s_p) = \exp(-2L/\pi s_p)$], we can eliminate the pressure p in the RTV scaling law and find the following expression for the density n_e ,

$$n_e = \frac{T_{max}^2}{2k_B L (1400 q_{Serio})^3 q_p} . \quad (9)$$

Inserting this density into the relation for the cooling delay (Eq. 4) we find indeed a proportional relation $\Delta t_{12} \propto L$,

$$\Delta t_{12} = L \times \left[\frac{6 (1400 q_{Serio})^3 q_p k_B^2 \ln \left(\frac{T_1}{T_2} \right)}{T_{max} \Lambda_{0,Ph} \alpha_{Fe}} \right] . \quad (10)$$

which should show up for cooling loops with similar maximum temperatures T_{max} . The relation $\tau_{cool} \propto L$ was also derived in Cargill et al. (1995; Eq. 14E therein) and Serio et al. (1991; Eq. 14 therein).

3. Data Analysis

We are using three data sets for which the cooling delay between the TRACE 195 Å and 171 Å filters has been measured: 11 nanoflare loops analyzed in Aschwanden et al. (2000), 4 medium-sized EUV loops analyzed in Schrijver (2002), and 5 large EUV loops analyzed in Winebarger et al. (2003).

In the first study (Aschwanden et al. 2000), nanoflare loops were measured on 1999 Febr 17, 02:15-03:00 UT, with a cadence of ≈ 2 min in both 171 Å and 195 Å with TRACE. The time delay between the appearance in the two filters was measured by cross-correlation of the two time profiles, shown in Fig.6 and listed in Table 1 of Aschwanden et al. (2000). The time delay was found to be positive in 11 out of 12 cases. We use only the 11 cases with positive time delay, sorted according to the loop length in Table 1. The loop length was determined from a geometric model of a projected semi-circular cylindrical loop. The electron density n_e is measured from the flux F_2 and loop width w according to Eq.(5).

In the second study (Schrijver 2001), time delays between the maximum intensity in the 171 and 195 Å TRACE passbands were measured in 4 active region loops observed above the limb on

2000 May 26. The loop half length was estimated with $L = (\pi/2)h + h_{limb}$ based on the height h of the loop top above the limb and a height correction $h_{limb} \approx 5$ Mm for the offset between optical limb and the portion of the plage inside the limb. The fluxes F_{171} and loop widths w could not be reliably measured for this subset, because of confusion problems in the crowded limb regions.

In the third study (Winebarger et al. 2002), 5 loops were measured on 1999 Aug 18, 1998 Jul 04, 1998 Jul 25, 1998 Aug 17, and 1998 Jul 25, in both the 171 Å and 195 Å filters with TRACE. The time delay between the two filters was measured from the peak times of asymmetric gaussian curves fitted to the light curves in the two filters. The loop lengths were measured from the best fit of elliptical and dipolar geometric models to the projected loop shapes.

Inserting the measured values F_2 , w , and Δt_{12} into Eq.(6) yields the iron abundance enhancement factors α_{Fe} listed in Table 1, which have a mean and standard deviation of $\alpha_{Fe} \leq 4.9 \pm 1.7$ for the dataset of Aschwanden et al. (2000), and $\alpha_{Fe} \leq 1.4 \pm 0.4$ for the dataset of Winebarger et al. (2003), respectively. Note that the mean iron enhancement is significantly higher for the small-scale nanoflares analyzed in Aschwanden et al. (2000) than for the large-scale loops of Winebarger et al. (2003). The variable degree of iron enhancement could be related to different physical conditions in freshly-filled small-scale loops compared with longer-lived large-scale loops. The effect of gravitational settling has been observed in observations of coronal streamers with SUMER (Feldman et al. 1999) and with UVCS (Raymond et al. 1997).

The values of α_{Fe} have to be considered as upper limits if the filling factor $q_w \leq 1$ is lower than unity. We can turn the argument around and assume that the iron abundance enhancement has to be larger than or equal unity, which would then constitute lower limits for the filling factors: $q_w \geq 0.23 \pm 0.08$ (Aschwanden et al. (2000) and $q_w \geq 0.78 \pm 0.22$ (Winebarger et al. (2003)).

Figure 1 shows the correlation plot between the cooling delay Δt_{12} and the loop half length L . A linear regression fit between the logarithmic values yields the power-law relation $\Delta t_{12} \propto L^{1.08 \pm 0.16}$ which is fully consistent with the theoretical prediction of a linear relationship $\Delta t_{12} \propto L^1$ (Eq. 10).

In order to verify our initial assumption of dominant radiative loss, we estimate also the conductive cooling time,

$$\tau_{cond} = \frac{3n_e k_B T_{max}}{\nabla F_C} = 1.1 \times 10^{-9} n_e T_{max}^{-5/2} L^2 , \quad (11)$$

where we assign a mean value of $T_{max} \approx 1.2$ MK for the looptop temperature, when the loop cools through the two TRACE passbands. The last two columns in Table 1 show that the conductive cooling time is always much larger than the radiative cooling time, $\tau_{cond} \gg \tau_{rad}$, which corroborates our a priori assumption of dominant radiative cooling.

4. Discussion

We have developed a simple method to constrain the iron abundance or filling factor in a coronal loop, based on the cooling delay measurement between two EUV filters. This model predicts a linear relationship between the cooling delay and the loop length, i.e. $\Delta t_{12} \propto L$, which is consistent with the observed relation, i.e. $\Delta t_{12} \propto L^{1.08 \pm 0.16}$.

The only underlying assumption is that the cooling is dominated by radiative loss in the temperature range of EUV loops ($T \approx 1.0 - 1.4$ MK here), rather than by conductive loss. Theoretical models of cooling in flare loops predict that conductive cooling is only dominant in the initial phase of very hot plasma seen in soft X-rays, say at $T \gtrsim 10$ MK, while the later cooling phase seen in EUV is dominated by radiative cooling (Antiochos 1980; Antiochos & Sturrock 1982; Cargill et al. 1995). Our measurements of the density allows us to estimate upper limits for the radiative cooling time. If there would be a filling factor $q_w < 1$, the density would be higher and the radiative cooling time shorter. But even for a filling factor of unity, we find that the radiative cooling time in the EUV temperature range is significantly shorter than the conductive cooling time, which corroborates our a priori assumption. This is also consistent with other observations of EUV loops, where the ratio of the cooling time to the radiative cooling time was found to be $\tau_{cool}/\tau_{rad} = 1.02$ (Aschwanden et al. 2000).

The main result of this study is the estimation of the iron abundance. We show a compilation of radiative loss functions in Fig. 2, which has been calculated for photospheric abundances (Meyer 1985), with an absolute iron abundance of $\log(A_{Fe}) = 7.59$ relative to hydrogen $\log(A_H) = 12.0$ (i.e. $A_{Fe}/A_H = 3.9 \times 10^{-5}$), as well as for coronal abundances (Feldman 1992), which have an iron enhancement by a factor of $\alpha_{Fe} = 3$. This enhancement factor of $\alpha_{Fe} = 3$ in density produces a change of the radiative loss rate that can be seen between the two curves calculated by Martens et al. (2000) in Fig. 2, at a temperature of $T \approx 1.0$ MK. Recent measurements of the absolute abundance of iron based on comparisons of EUV and radio data yielded a value of $A_{Fe}/A_H = 1.56 \times 10^{-4}$, or a coronal iron enhancement by a factor of $\alpha_{Fe} = 4.0$ (White et al. 2000). Our measurements from 16 different loops in many different active regions yield a median value of $\alpha_{Fe} = 4.0$, or a mean and standard deviation of $\alpha_{Fe} = 3.7 \pm 2.2$. Because of this reasonable agreement of iron enhancements with radio methods (White et al. 2000) and spectroscopic measurements (Feldman 1992), our result corroborates the notion that low-FIP elements such as Fe are enhanced in the corona relative to photospheric values (Feldman 1992). By the same token we can argue the filling factor is close to unity in coronal EUV loops, otherwise we would have disagreement with spectroscopic and radio iron abundance measurements.

Acknowledgements: Part of this work was supported by NASA contracts NAS5-38099 (TRACE) and NAS8-00119 (SXT).

References

Antiochos,S.K. 1980, ApJ 241, 385

Antiochos,S.K. & Sturrock,P.A. 1982, ApJ 254, 343.

Aschwanden,M.J., Tarbell,T.T., Nightingale,W., Schrijver,C.J., Title,A., Kankelborg,C.C., Martens,P., and Warren,H.P. 2000, ApJ 535, 1047

Aschwanden,M.J. and Schrijver,C.J. 2002, ApJS, 142, 269

Cargill,P.J., Mariska,J.T., and Antiochos,S.K. 1995, ApJ 439, 1034

Cook,J.W., Cheng,C.C., Jacobs,V.L., and Antiochos,S.K. 1989, ApJ 338, 1176

Feldman,U. 1992, Physica Scripta 46, 202

Feldman,U., Doschek,G.A., Schühle,U., and Wilhelm,K. 1999, ApJ 518, 500.

Golub,L. and Pasachoff,J.M. 1997, *The Solar Corona*, Cambridge: Cambridge University Press

Martens,P.C.H., Kankelborg,C.C., and Berger,T.E. 2000, ApJ 537, 471

Meyer,J.-P. 1985, ApJS 57, 173

Raymond,J.C. and 26 co-authors 1997, Solar Phys. 170, 105,

Rosner,R., Tucker,W.H., and Vaiana,G.S. 1978, ApJ 220, 643

Schrijver,C.J. 2001, Solar Phys. 198, 325

Schrijver,C.J. and Zwaan,C. 2000, *Solar and stellar magnetic activity*, 2000, Cambridge: Cambridge University Press

Serio,S., Peres,G., Vaiana,G.S., Golub,L., and Rosner,R. 1978, ApJ 243, 288

Serio,S., Reale,F., Jakimiec,J., Sylwester,B., and Sylwester,J. 1991, AA 241, 197.

Warren,H.P., Winebarger,A.R., and Mariska,J.T. 2003, ApJ, (subm.)

White,S.M., Thomas,R.J., Brosius,J.W., and Kundu,M.R. 2000, ApJ 534, L203

Winebarger,A.R., Warren,H.P., and Seaton,D.B. 2003, ApJ, (subm.)

Table 1. Cooling delays and iron abundances inferred from observations with TRACE ([A]=Aschwanden et al. (2000), [S]=Schrijver (2001), and [W]=Winebarger et al. (2003).

No.	Loop	Flux	Width	Length	Time	Electron	Iron	Radiative	Conductive
		#	F_{171} [DN/s]	w [Mm]	L [Mm]	Δt [min]	n_e [10^9 cm^{-3}]	α_{Fe}	τ_{rad} [min]
1	#8 [A]	23.30	6.1	19.4	2.53	3.2	4.2	6.7	141.2
2	#10 [A]	38.97	2.2	6.0	1.12	7.0	3.0	3.0	29.1
3	#12 [A]	26.84	2.3	5.8	3.01	5.6	2.2	8.0	22.1
4	#16 [A]	21.08	3.5	9.9	1.76	4.0	4.0	4.7	46.2
5	#20 [A]	19.67	5.1	15.9	0.82	3.2	7.4	2.2	95.3
6	#55 [A]	14.19	7.2	14.5	0.61	2.3	12.0	1.6	56.7
7	#73 [A]	14.00	3.2	12.7	0.89	3.5	6.7	2.4	64.8
8	#190 [A]	15.41	2.9	7.4	0.76	3.8	6.6	2.0	24.2
9	#256 [A]	14.69	1.8	2.9	0.86	4.7	5.0	2.3	4.6
10	#315 [A]	15.82	2.9	13.1	1.61	3.9	4.5	4.3	76.9
11	#380 [A]	16.28	1.8	2.9	0.68	5.0	5.3	1.8	4.9
12	#21 [S]	–	–	32.0	4.2	–	–	–	–
13	#54 [S]	–	–	33.0	4.2	–	–	–	–
14	#86 [S]	–	–	41.0	4.2	–	–	–	–
15	#120 [S]	–	–	45.0	3.3	–	–	–	–
16	#1 [W]	38.24	2.2	13.0	2.50	6.9	2.0	6.6	135.2
17	#2 [W]	8.85	3.2	65.0	23.3	2.8	1.6	61.8	1350.0
19	#3 [W]	36.69	5.5	102.0	23.3	4.3	1.1	61.8	5160.0
18	#4 [W]	30.48	3.0	78.0	10.0	5.3	1.3	26.5	3720.0
20	#5 [W]	9.16	12.0	178.0	183.0	1.4	1.1	485.8	5310.0

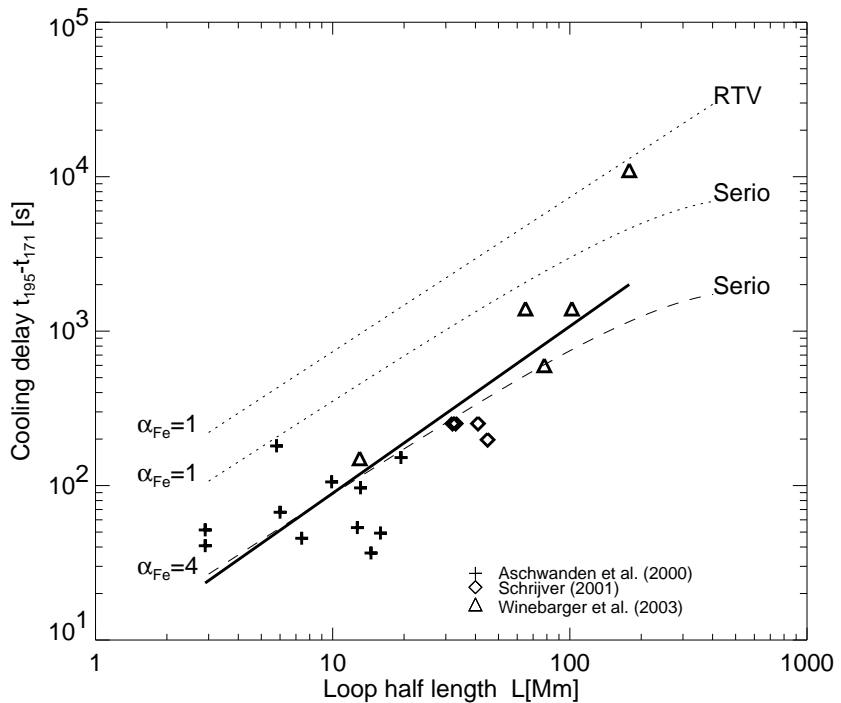


Fig. 1.— Cooling delays Δt_{12} are measured between the peak time in the TRACE 195 Å and 171 Å filters, as function of the loop half length L , from three datasets with 11 nanoflare loops (crosses; Aschwanden et al. 2000), 4 active region loops (diamonds; Schrijver 2002), and 5 active region loops (triangles; Winebarger et al. 1003). The thick line represents a linear regression fit with a slope of 1.08 ± 0.16 . The theoretically predicted scaling laws (based on RTV and Serio et al.) are shown for an iron enhancement factor of $\alpha_{Fe} = 1.0$ (dotted) and $\alpha_{Fe} = 4.0$ (dashed).

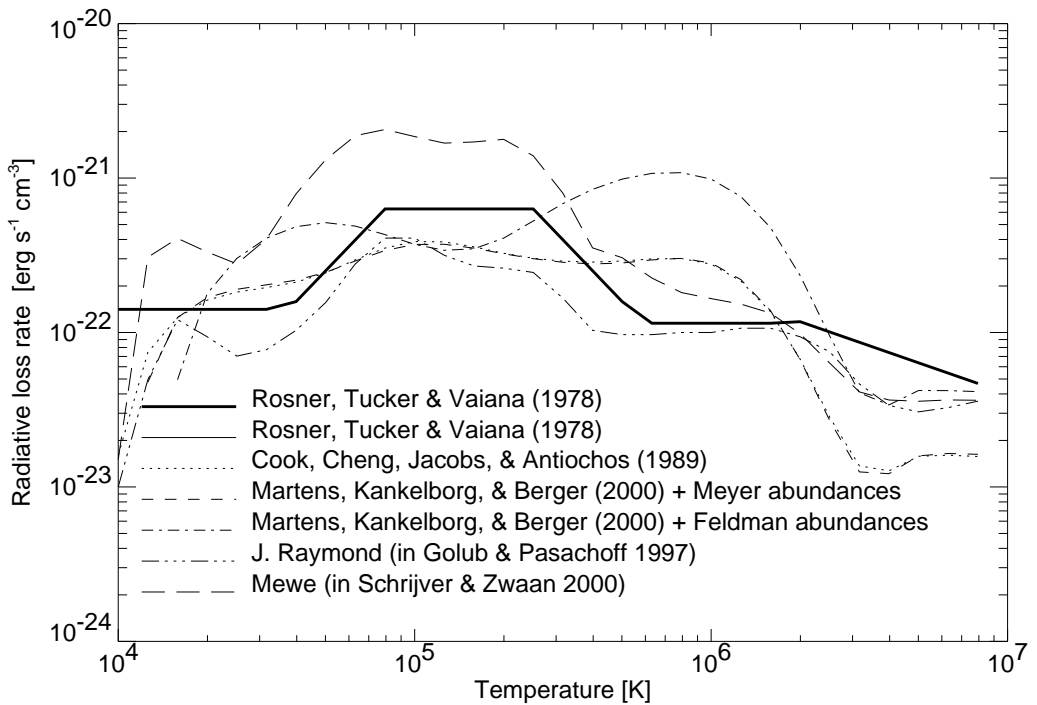


Fig. 2.— A compilation of radiative loss functions is shown. The differences mainly result from the assumptions of elemental abundances. Coronal abundances (e.g. Feldman 1992) have a ≈ 3 times higher iron content than photospheric abundances (e.g. Meyer 1985), and thus increases the value of the radiative loss function by the same factor at temperatures around $T \approx 0.5 - 2.0$ MK. The one-piece powerlaw approximation is used in the derivation of the RTV scaling law.